Journal of
Mechanics of
Materials and Structures

A NEW EARTHQUAKE-RESISTANT CONCRETE FRAME WITH FIBER-REINFORCED PLASTIC FABRICS AND SHIFTED PLASTIC HINGES

M. Saiid Saiidi, Erik Reinhardt and Faramarz Gordaninejad

Volume 4, Nº 5 May 2009

mathematical sciences publishers

JOURNAL OF MECHANICS OF MATERIALS AND STRUCTURES
Vol. 4, No. 5, 2009

A NEW EARTHQUAKE-RESISTANT CONCRETE FRAME WITH FIBER-REINFORCED PLASTIC FABRICS AND SHIFTED PLASTIC HINGES

M. SAIID SAIIDI, ERIK REINHARDT AND FARAMARZ GORDANINEJAD

An innovative structural pier employing concrete, steel, and carbon fiber composite sheets was developed and implemented in a two-column bridge pier. The basic concept for the pier design is that the pier has preassigned plastic hinges in the columns. Outside the plastic hinges, the pier is to remain elastic. The innovative concept incorporated in the pier is that where plastic hinging and ductility is required, steel reinforcement is used as longitudinal reinforcement, and where elastic behavior is required, carbon-fiber-reinforced plastic (CFRP) sheets are used as longitudinal reinforcement. Confinement and shear capacity are provided for by fiber-reinforced polymer sheets at all locations. The pier is detailed so that the plastic hinges are shifted away from the column ends because shifted plastic hinges prevent damage from penetrating into the joint area and are easier to repair. A quarter-scale, two-column pier with square columns was designed and constructed based on the aforementioned concept. Ordinary concrete and mild steel were used in the pier. A unidirectional carbon composite was placed on the pier. The pier was studied using computer programs DRAIN 3-DX and RC-Shake and a shake table testing program was developed. The pier was subjected to successive runs of the 1994 Northridge–Sylmar record with increasing amplitudes until failure. The plastic hinges behaved as planned, and the failure occurred after the rupture of the CFRP confinement sheets at one of the plastic hinges. There was no apparent damage outside the plastic hinges. Extensive nonlinear analytical studies using multiple- and single-degree-of-freedom modes were conducted and the results were compared with the measured response. It was found that both models were generally capable of reproducing the experimental results.

1. Introduction

Applications of fiber-reinforced polymer (FRP) fabrics in civil infrastructure systems have been mainly in retrofits or repairs of substandard or damaged reinforced concrete structures [Teng et al. 2001]. FRP fabrics have rarely been used in new construction. In contrast, FRP members in the form of concrete filled tubes or FRP beams attached to concrete slabs have been investigated for use in new construction [Saiidi et al. 1994; Mirmiran et al. 2000]. The primary benefits of FRP materials are realized regardless of whether FRP fabrics or members are used. The high strength and ease of installation are generally the most important characteristics of FRPs. One characteristic of FRPs that could limit their application for certain uses is the lack of ductility in FRP fabrics and members when used by themselves. However, the linear behavior of FRP materials up to failure in combination with their high strength can be a feature that can be taken advantage of in structures where nonlinear behavior is not desired.

Current seismic design provisions for standard (noncritical) structural systems envision significant nonlinear deformations at preassigned locations in the structure. In building frames, the typical location for plastic hinges is at beam ends, whereas in bridges plastic hinges are expected at column ends. The

Keywords: bridges, carbon fiber, earthquake, nonlinear analysis, offset hinges, piers, shake table testing.

structure outside the plastic hinges is expected to remain elastic. This requirement can be satisfied by FRPs. The study presented here is aimed at developing and investigating a novel construction method for bridge piers in which FRP fabrics provide the primary longitudinal and transverse reinforcement in all segments of the pier except for the column plastic hinges where energy dissipation is expected. At the plastic hinges, conventional steel bars are used as longitudinal reinforcement and FRP fabrics are used as transverse reinforcement. An added feature of the proposed construction is the shifting of plastic hinges away from but close to the column ends, a concept that has been attempted in conventional reinforced concrete buildings but not bridges [Galunic et al. 1977; Abdel-Fattah and Wight 1987]. This article presents a summary of the concept, the design, construction, and shake table testing of a two-column pier utilizing this concept, measured data, and analytical studies of the new pier. Details of the study are presented in [Reinhardt et al. 2003].

2. Pier details

The proposed pier is a concrete structure with a very small amount of longitudinal and transverse steel reinforcement in all locations except for the column plastic hinges. Consistent with the practice of strong pier caps in bridge engineering, plastic hinging of the beams is precluded. In the column plastic hinges, longitudinal steel reinforcement is provided to dissipate the earthquake energy. However, confinement and shear capacity in the plastic hinges is provided by unidirectional FRP fabrics. The longitudinal and transverse reinforcement in the beam and the elastic portions of the columns are also provided by unidirectional FRP fabrics.

To evaluate the feasibility and seismic performance of the proposed structure, a two-column pier was constructed, reinforced with very low steel reinforcement ratios and carbon-fiber-reinforced plastic (CFRP) laminates, and tested to failure on a shake table. The test pier was a $1/4$ scale model of a typical reinforced concrete bridge pier. Figure 1 shows the pier dimensions and the composite layout. The lines

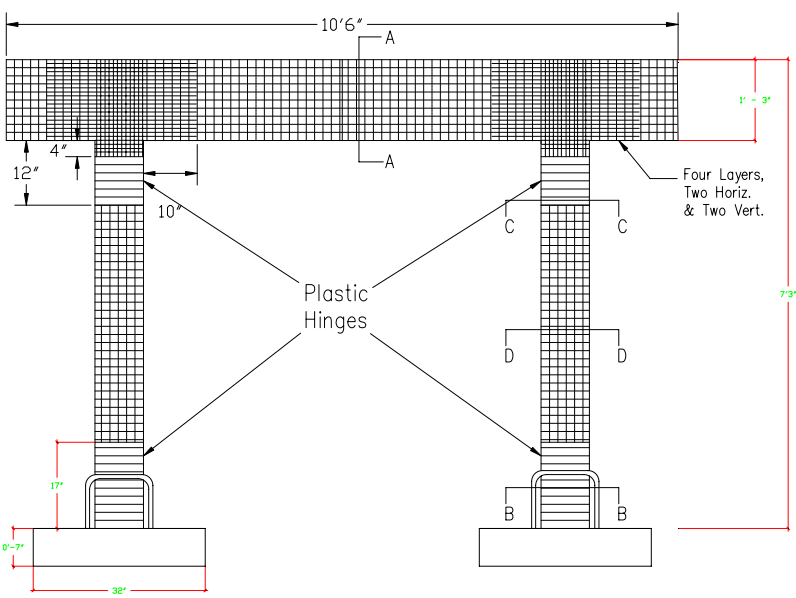

Figure 1. Dimensions of pier and arrangement of composites.

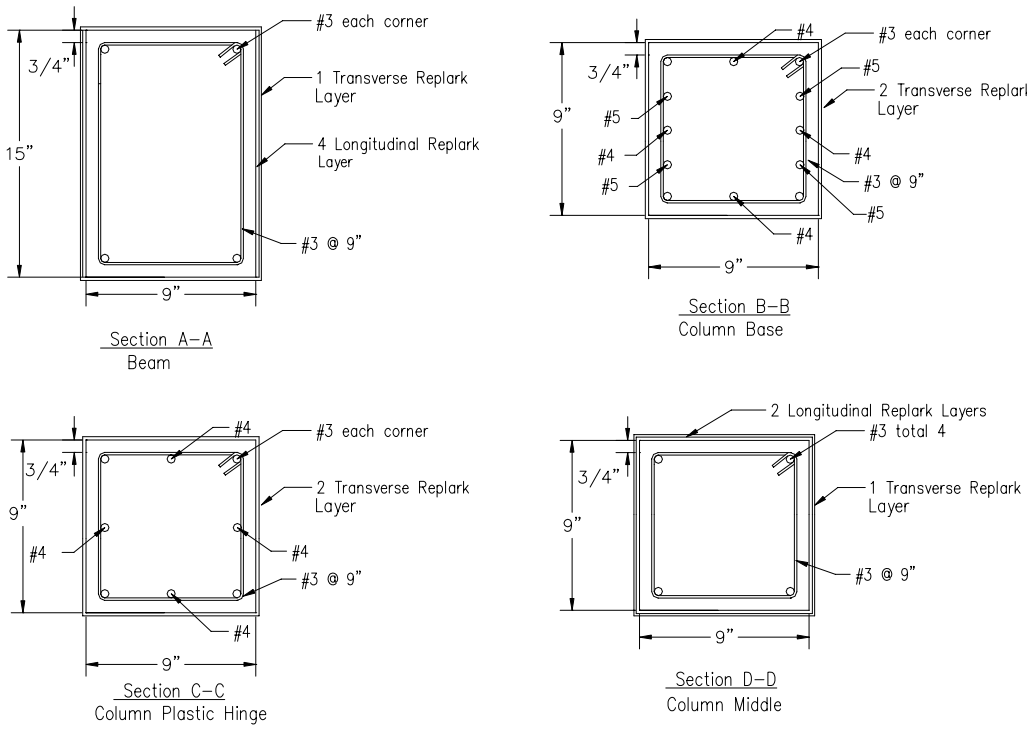

Figure 2. Pier section details and composite layout.

within the elements show the direction of the carbon fibers. Figure 2 shows the bent cap and column cross-sections. The design criterion for the steel reinforcement outside the plastic hinges was for the concrete members to resist self weight. Other considerations were one bar at each corner and small diameter tie and stirrups at a spacing of approximately the minimum member cross sectional dimension.

Another feature of the proposed pier is that the plastic hinges are offset relative to the ends of the column. In a prototype, the shifting would facilitate repair and inspection of the plastic hinges after strong earthquakes. To shift the plastic hinges, a relatively high amount of steel was used at the column ends to ensure that they remained elastic (see Section B-B in Figure 2). Two horizontal and two vertical layers of CFRPs were provided on each side of the joints as shear reinforcement. The joint shear design was based on the ACI 352 provisions [Mirmiran et al. 2000].

Normal-weight concrete with a maximum aggregate size of 10 mm (3/8 in) was used. The target concrete compressive strength was 5 ksi (34 MPa), while the actual strengths were 6.26 ksi (42.8 MPa) in the columns and 5.29 ksi (36.1 MPa) in the bent cap on the day of testing. The concrete was air cured, and subsequently the surface of the concrete was prepared for laminate application. The specified grade of the steel reinforcement was 60. The measured yield stresses for the #3, #4, and #5 bars were, respectively, 66.3, 63.3, and 65.0 ksi (453, 432, and 444 MPa). The Mitsubishi CFRP product, Replark Type 30, was used. First the surface was ground using a disk grinder, then putty (supplied by the manufacturer of the composites) was applied to smooth out rough areas. Next, a layer of resin undercoat was applied followed by a layer of carbon fiber sheet. This was repeated as needed, and the process was completed by

application of a resin overcoat. Any air bubbles trapped beneath the laminate were repaired by injecting epoxy into the voids.

Per the manufacturer the lamina elastic modulus was 33,400 ksi (228 GPa) and its tensile strength was 493 ksi (3.365 GPa) in the fiber direction. One inch (25.4 mm) coupons were tested as part of the study. The measured lamina elastic modulus in the fiber direction was 38,400 ksi (262.3 GPa) and its tensile strength was 379.8 ksi (2.593 GPa). The measured lamina elastic modulus was 509.6 ksi (3.48 GPa) and its tensile strength was 1.76 ksi (12 MPa) perpendicular to the fiber direction.

Three configurations of the footings were used in the study: (1) as-built, flexible; (2) retrofitted, flexible; and (3) fixed. The first and second configurations were necessary for low-amplitude studies of the effect of footing flexibility in the linear range. The maximum longitudinal bar strains during that part of the study were kept below two-thirds of the measured steel yield strain. The results of the low-amplitude studies were presented elsewhere [Saiidi et al. 2002]. The subject of the present paper is the fixed footing configuration. The pier model was designated as B2SF for bent with 2 square columns and fixed footings. [Reinhardt et al. 2003] provides more details about the study.

3. Shake table tests

The test setup is shown in Figure 3. The footings were fixed to a 14.5 ft × 15 ft (4.42 m × 4.57 m) shake table using steel brackets and threaded bars. The bent was extensively instrumented with strain gages, displacement transducers (to measure displacements and curvatures), accelerometers, and a load cell (to measure lateral load applied to the specimen).

The target column axial load index (ALI, defined as the percent ratio of the axial load and the product of the gross area and the target concrete compressive strength) was 8%. The range of ALI in bridge columns is typically 5 to 10%. The uniform vertical load on the cap beam to produce an ALI of 8% was

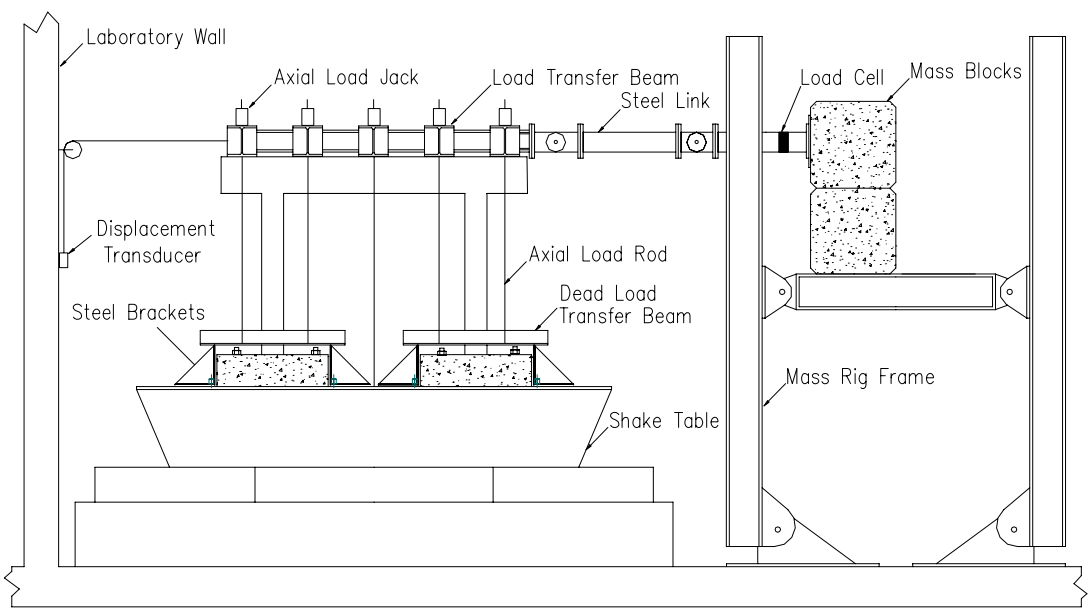

Figure 3. Shake table test setup for fixed-base model.

6.1 kip/ft (88.6 kN/m). The vertical loading was accomplished using five pairs of threaded bars running between the transfer beam and the footings each stressed to 6.4 kip (28.5 kN) using hydraulic rams (see Figure 3). A system of accumulators was attached to the rams to minimize axial load fluctuation caused by the extension of the threaded bars during earthquake simulations. To replicate the inertial effect of the gravity loads, a mass rig was used, which consisted of a pinned steel frame mechanism supporting concrete reaction blocks. The mass rig had an effective lateral inertial load of 64 kip (285 kN) and was connected to the loading frame by a pinned rectangular steel tube.

The earthquake history used to drive the shake table was the January 17, 1994 Northridge earthquake as measured at the Sylmar Hospital station. The peak ground acceleration of this record is 0.61 g. This record was chosen due to its being representative of typical earthquakes in the Western United States. Furthermore, preliminary analytical studies showed that this record would lead to high ductility demand thus allowing for ultimate behavior testing. Since the test specimen was a scaled model of the prototype column, the earthquake record time axis was scaled by a factor of 0.5 to create a response in the test specimen that would represent the prototype response. The pier was subjected to scaled versions of the Sylmar record in 13 simulations (runs), beginning with several preyield runs and continuing until pier failure. Intermittent low-amplitude quick release tests were conducted to measure the effective period and damping of the bent.

Table 1 shows the target peak table accelerations (PTAs) for different runs. The fine increments in the first six runs were necessary for the evaluation of the footing flexibility effects reported in [Saiidi et al. 2002]. The peak target accelerations were 0.36 g and 0.24 g in the as-built and retrofitted footing configurations, respectively [Saiidi et al. 2002]. The actual peak accelerations were within 5% of the target values. The increment in run 12 was small because failure appeared to be imminent. However, it took an additional motion with a slightly higher PTA to cause the pier to fail. During the postyield runs the actual PTAs were within 10% of the target values.

Run number	Motion	Peak table acceleration (g)
1	0.1 × Sylmar	0.06
2	0.2 × Sylmar	0.12
3	0.3 × Sylmar	0.18
4	0.4 × Sylmar	0.24
5	0.5 × Sylmar	0.30
6	0.6 × Sylmar	0.36
7	0.8 × Sylmar	0.48
8	1.0 × Sylmar	0.60
9	1.25 × Sylmar	0.75
10	1.50 × Sylmar	0.90
11	1.75 × Sylmar	1.05
12	1.90 × Sylmar	1.14
13	2.00 × Sylmar	1.20

Table 1. Earthquake simulation protocol for B2SF.

4. Test results

The testing of the fixed footing configuration (3) was conducted after the pier had been subjected to low-amplitude motions. The maximum measured longitudinal bar strains for configurations (1) and (2) were 67% and 60% of the yield strains, respectively. The initial stiffness data indicated some softening due to minor cracking, but cracks were not visible and there were no signs of damage. The key response parameters that were evaluated to judge the performance of the pier were: observed damage, displacements, curvatures, and strains.

Observed damage. During the first two runs (see Table 1), no damage was visible. Under run 3 (with PTA of 0.18 g), horizontal cracks were seen in the transverse layer of composites at the bottom of the columns. In subsequent runs these cracks widened slightly and new thin horizontal cracks in the epoxy resin were visible. Multiple epoxy cracking noises could be heard in these runs. After run 11 (PTA of 1.05 g), a crack in the concrete at the right beam-column joint was noted. The bent appeared to be stable, but large and increasing movements were of concern. As a result the increment for the following run (run 12) was reduced. More cracking of the epoxy was noted during this run without any notable further damage. During the following run, with a peak acceleration of 1.2 g, a part of the confinement composite layer failed near the bottom of the right column in the plastic hinge region (see Figure 4). Also, the confinement composite jacket at the top of the right column delaminated from the concrete. Testing was terminated after this run due to the failure of the composite jacket and a drop in the lateral load capacity.

Lateral displacement response. Figure 5 shows the cumulative force-displacement hysteresis curve. The first few input motions resulted in mostly linear response. At larger PTAs, nonlinear loops were developed. Run 7 with a target PTA of 0.48 g led to a maximum lateral displacement of 1.1 in (28 mm) or

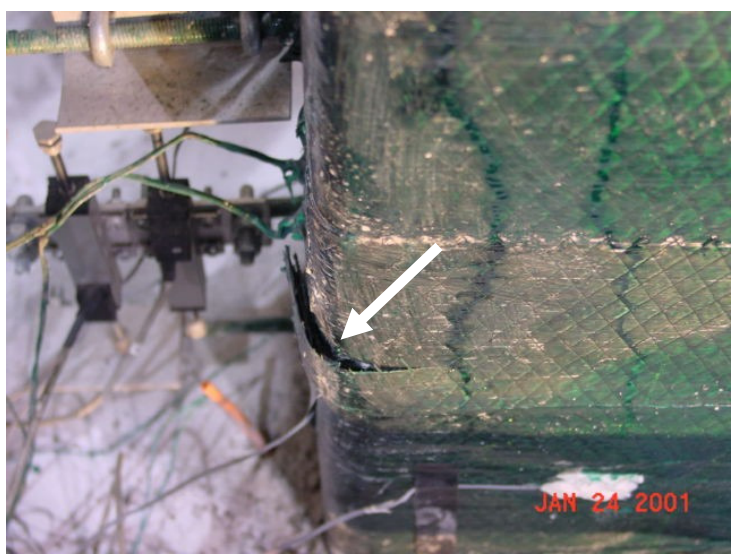

Figure 4. Ruptured jacket at bottom plastic hinge of right column.

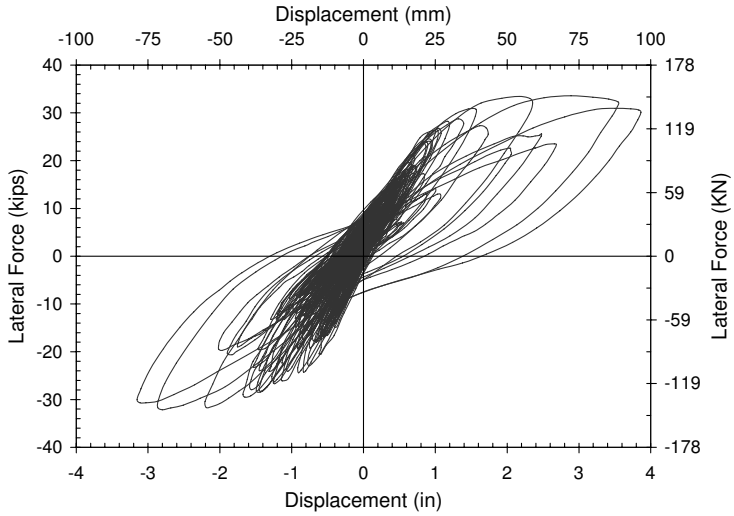

Figure 5. Cumulative measured force-displacement relationship.

approximately 1.5% drift. Subsequent runs led to relatively large-amplitude hysteresis loops and extensive nonlinear deformations. The hysteresis loops were relatively wide and indicative of large energy dissipation. The shifted plastic hinges were effective in providing the mechanism for energy dissipation and ductility.

The envelope of the measured force-displacement relationships for the primary direction of motion (the positive displacement range in Figure 5) is shown in Figure 6. It can be seen that stiffness reduced

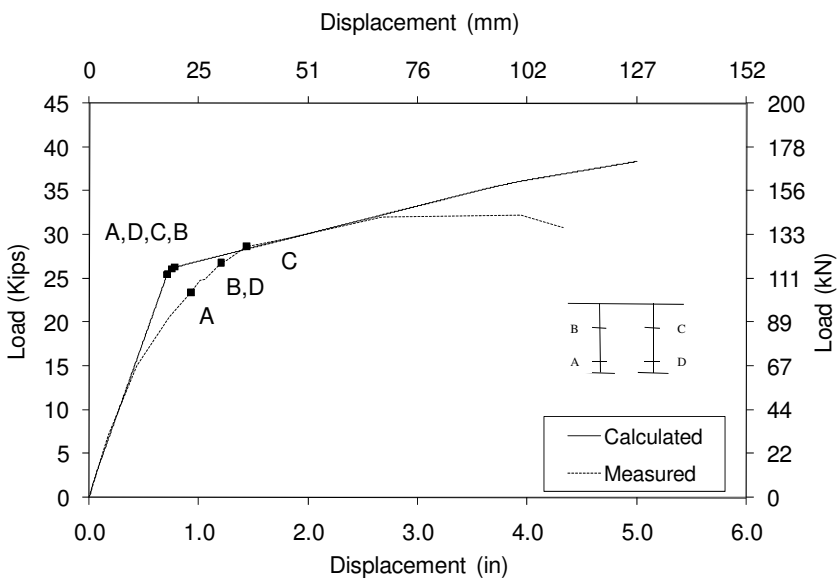

Figure 6. Force-displacement envelope: calculated values (upper curve) and measured ones (lower curve).

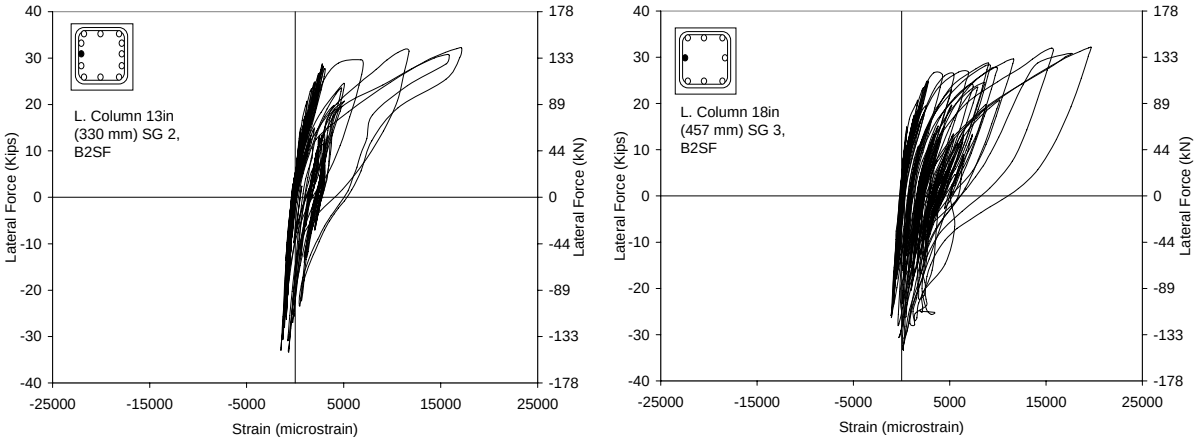

Figure 7. Force-strain relationship outside (left graph) and inside (right graph) the lower left column plastic hinge.

progressively with increasing level of acceleration, indicating gradual yielding at the hinges. Slight nonlinearity was observed in the first 7 runs, corresponding to displacements up to 1.05 in (26.7 mm). The source of the nonlinearity was primarily concrete deformation. The lateral load capacity did not change significantly during Runs 10–13, corresponding to displacements of 2.2 in (56 mm) to failure. During Run 13 when the FRP jacket failed the peak lateral force dropped by approximately 10%.

Based on an elastoplastic idealization of the measured envelope the measured effective yield displacement was 0.7 in (17.8 mm). At the first sign of failure the ductility capacity was 5.6, which exceeds the target ductility capacity of 4 or 5 used in practice. The drift capacity of the bent was 5.4%, which is also indicative of ample deformability of the proposed bent. The ductility and drift capacity of the proposed pier were close to the corresponding capacities of a conventional bridge bent with similar aspect ratio that was tested in a previous study [Moustafa et al. 2004] and labeled "B2CM" there.

Strains. The maximum strains in the column plastic hinge steel bars were approximately 20,000 microstrains at about 8 in (200 mm) below the bottom of bent cap and 8 in (200 mm) above top of footings. The peak strains in the column bars immediately below the bottom of the bent cap and immediately above the footings were less than these values demonstrating that the plastic hinges were indeed formed away from the ends as intended. Figure 7 shows sample strain data as a function of the pier lateral force for column bars outside and inside the plastic hinge near the bottom of the left column. Note some yielding of the longitudinal bars spread outside the plastic hinge. This is attributed to strain hardening of the bars inside the plastic hinge. Peak strains in the bent cap bars were approximately 3000 microstrains, indicating that the bent cap steel bars experienced limited yielding (the measured yield strain for the bars was 2190 microstrains).

The maximum measured strain on the transverse FRP layers on the column plastic hinges was approximately 4000 microstrains and was far less than the design strain of 10800 microstrains. As stated earlier, the transverse FRP layers eventually failed. However, there were no strain gages at the failure location and the actual strain could not be measured. The tensile strains in the longitudinal FRP layers

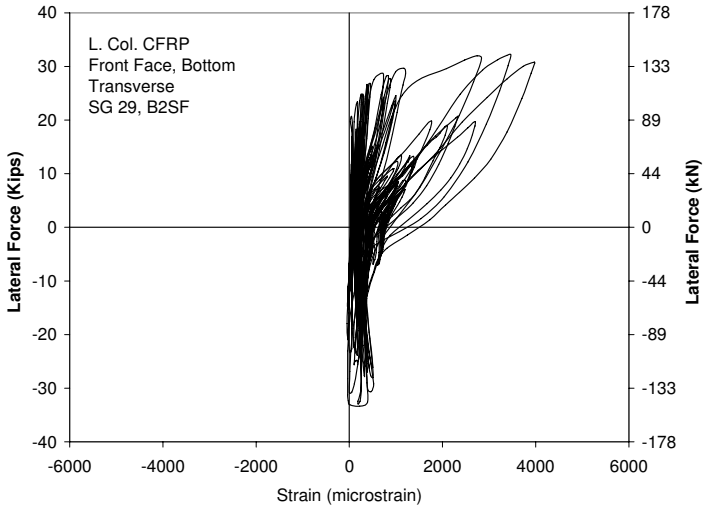

Figure 8. Force-transverse strain relationship on FRP at the lower left column plastic hinge.

parallel to the column axes were close to 4000 microstrains, well below the design strain of 10800 microstrains. Figure 8 shows a sample measured pier force-strain relationship for the transverse direction. The maximum strain in the composite layers on the bent cap parallel to the bent cap axis was less than 3000 microstrains, implying that the bent cap composite fabrics did not suffer any damage, as intended. Also, the maximum strain in the composite fabrics perpendicular to the bent cap, which were used for shear reinforcement, was approximately 1500 microstrains, meaning that the bent cap shear design was adequate. The maximum fabric strain in the joint region was close to 1000 microstrains. However, upon removal of the composite layer after the final shake table test, cracks were seen in the joint indicating that the joint design procedure may need to be reevaluated for possible increase in the number of fabric layers.

The composite fabrics were removed after the test to survey the damage locations and evaluate crack patterns. Horizontal cracks were noted at the plastic hinge region, which was to be expected because no vertical composite fibers were present in this area (see Figure 9). However, a number of shear cracks at approximately 40° to the horizontal were noted in the plastic hinges in the right column. These cracks are believed to have formed after the confinement CFRP ruptured. Shear cracks were also visible in the joint region, as shown in Figure 9, which suggests that additional CFRP layers may be necessary.

The composite layers in the bent cap and the portion of the columns in between plastic hinges did not delaminate, indicating that these regions remained elastic as was intended.

5. Analytical studies

The analytical studies consisted of nonlinear dynamic analysis of the test model using a multiple-degree-of-freedom (MDOF) and a single-degree-of-freedom (SDOF) model. The objective was to determine the adequacy of the modeling techniques used in detailed MDOF models and in simplified global SDOF models. More details of the analytical studies are presented in [Reinhardt et al. 2003].

MDOF modeling. The computer program DRAIN-3DX was used for the detailed representation of the test pier and for conducting nonlinear static and dynamic analyses of the test pier [Prakash et al. 1994]. Figure 10 shows the location of the nodes and elements in the analytical model. Linear beam-column elements were used outside the plastic hinges, and cracked section properties were used for the linear elements. A lumped plasticity moment rotation element was assigned to each plastic hinge. The hysteretic response of the plastic hinges was represented by the Takeda model. This model was developed to represent the cyclic response of reinforced concrete elements confined with steel reinforcement and accounts for the degradation of stiffness as cracking and yielding occurs. In the absence of a more specific model, it was assumed that the Takeda model is applicable to the plastic hinges in the test pier, even though the confinement in the test pier was provided by CFRP rather than steel reinforcement.

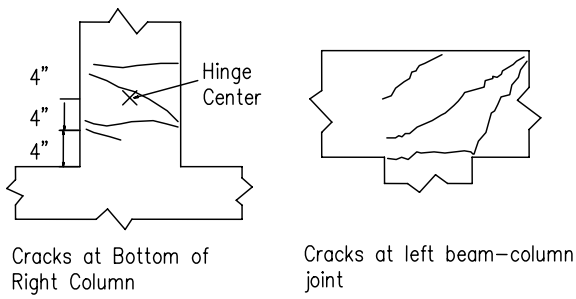

Figure 9. Postfailure crack patterns.

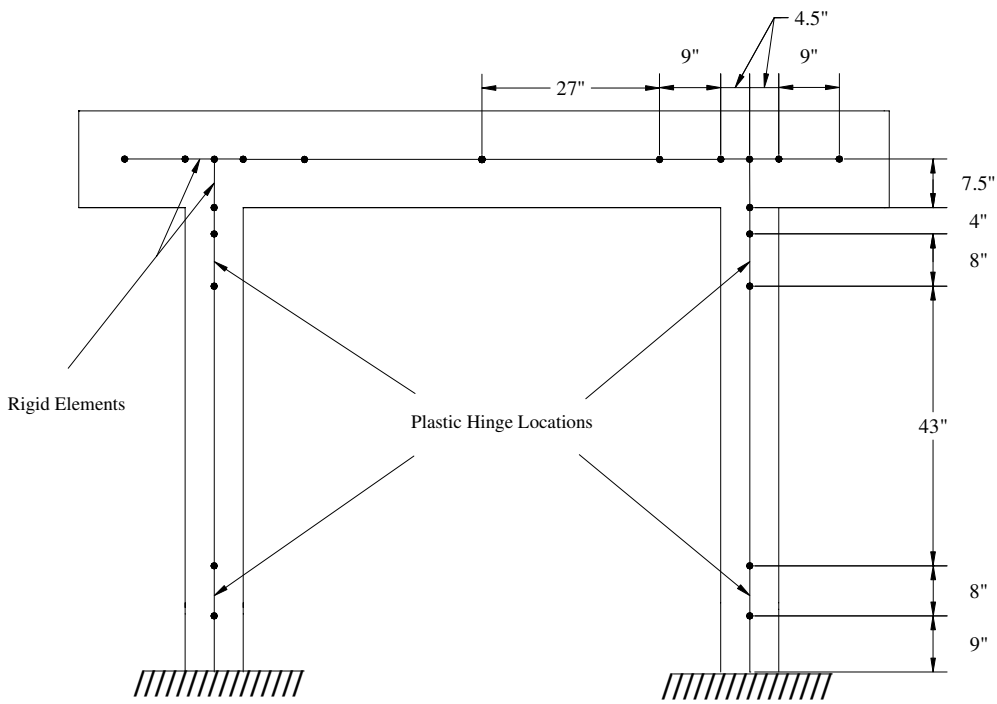

Figure 10. DRAIN-3DX model of the pier.

Results from MDOF analysis. The nonlinear static analysis of the test pier under lateral load was carried out under increasing displacements up a lateral drift ratio of 6%. Figure 6 shows the results of the analysis and comparison with experimental data. It is evident that the correlation between the measured and calculated curves was close. The initial stiffness values from the two curves were within 2% of each other. The calculated plastic hinging occurred at the same point marked A through D and presented a clear, sharp yield point. The measured longitudinal bar strains in the plastic hinges showed a more gradual yielding reflecting variation in the axial load between the two columns and perhaps material variability and slight deviation from the planned location of the bars. The postyielding slope of the calculated curves was close to the measured slope except at larger displacements. The difference is attributed to the fact that the analytical model did not include strength degradation effects, whereas in the actual pier there was some degradation of concrete strength at larger displacements. Altogether the correlation between the calculated and measured static lateral load analysis results was close and satisfactory.

To evaluate the performance of the dynamic analytical model in duplicating the measured results, the calculated and measured displacement histories for different shake table earthquake runs were compared. The actual shake table acceleration records were used in the analysis. The input record used in the analysis was the compilation of all the earthquake simulations that had been applied to the test model, spliced to ensure that the accumulated damaging effects of different earthquakes were accounted for. Intermittent free vibration tests of the pier were not included in the input motion because they are of very small amplitudes having negligible effect. The free vibration tests had shown that the effective damping ratio was 2%. However, the damping ratio typically assumed for reinforced concrete (RC) structures is 5%. The analysis of the pier was conducted for both 2% and 5% damping ratios and the results were compared with the measured displacement histories.

Figures 11 and 12 show sample results comparing the calculated and measured displacement histories for 1 × Sylmar and 1.75 × Sylmar motions, respectively. The former corresponds to a relatively small level of nonlinearity at 2% maximum drift and the other is associated with a relatively high nonlinearity at 4.4% maximum drift. A reasonably close agreement can be observed between the measured and calculated results for both damping ratios in both figures in terms of the waveforms and amplitudes. For both earthquakes the calculated results for 2% damping showed better correlation with the test data than the results with 5% damping did. The damping ratio of the test pier was lower than the ratio normally

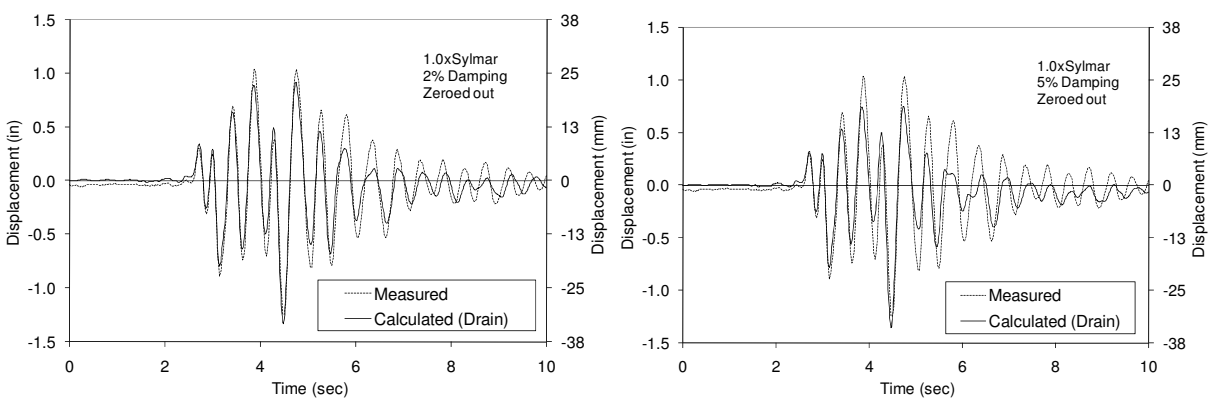

Figure 11. Measured and DRAIN-3DX results for 2% and 5% damping under 1 × Sylmar.

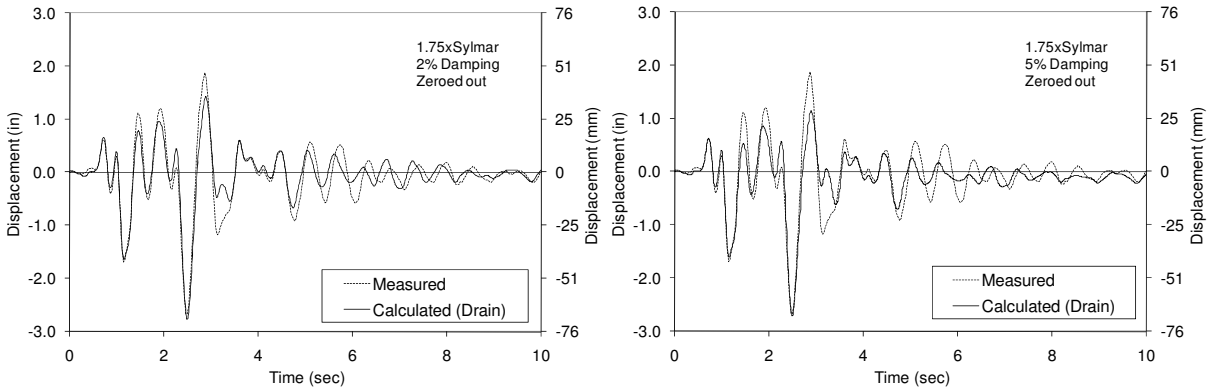

Figure 12. Measured and DRAIN-3DX results for 2% and 5% damping under 1.75 × Sylmar.

attributed to RC structures because the test pier did not include any nonstructural members that usually add to the overall damping of structures. Under 1 × Sylmar the calculated peak displacements were lower than the measured displacements by 6.9% and 8.4% for the 2% and 5% damping analyses, respectively. The differences for the 1.75 × Sylmar motion were lower at 3.6% and 1.4% for the 2% and 5% damping analyses, respectively.

SDOF modeling. The SDOF idealization of the test pier was carried out using the program RC-Shake [Saiidi 1982]. This is a computer program that calculates the dynamic response of a structure modeled as a SDOF nonlinear system, considering both hysteretic and viscous damping, as well as the loading setup of the mass rig system used in shake table testing. A degrading stiffness hysteresis model, called Q-hyst, characterizes the nonlinear load-deformation response [Saiidi 1982]. The input to the program requires a bilinear load-displacement relationship. The calculated nonlinear static analysis results obtained from DRAIN-3DX were used for this purpose. Because Q-hyst operates on a bilinear force-displacement relationship, it assumes that the system is already cracked. As a result the results from RC-Shake do not represent the low-amplitude, uncracked response of the structure. The output of the program provides the force and displacement histories of the SDOF system.

Results from SDOF analysis. RC-Shake was used to analyze the pier subjected to the measured acceleration histories collected during shake table tests. The acceleration records for all the earthquake simulation runs were spliced and used in the analysis. Response histories were calculated for both 2% and 5% damping. The results for 1 × Sylmar and 1.75 × Sylmar are shown in the next two figures. Figure 13 shows that the correlation between the measured and calculated results was excellent. The results for the 2% damping ratio were slightly better in duplicating the amplitudes in the second half of the response indicating that the 5% damping ratio overestimated the actual viscous damping. Under 1 × Sylmar the calculated peak displacements were lower than the measured displacements by 8.1% and 7.1% for the 2% and 5% damping analyses, respectively. Comparing Figures 13 and 11 reveals that the correlation between the RC-Shake results and the measured data was better than that between the DRAIN-3DX results and the measured displacements. The correlation between the calculated and measured results for 1.75 × Sylmar was also close, although the peak displacements were overestimated by 26% and 13% for the 2% and 5% damping, respectively (see Figure 14). In Figure 14 it can be observed that the calculated

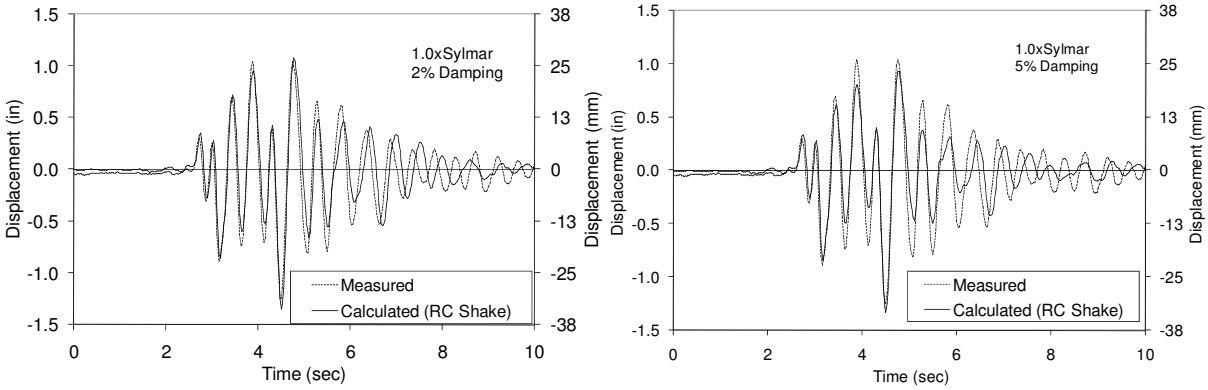

Figure 13. Measured and RC-shake results for 2% and 5% damping under 1 × Sylmar.

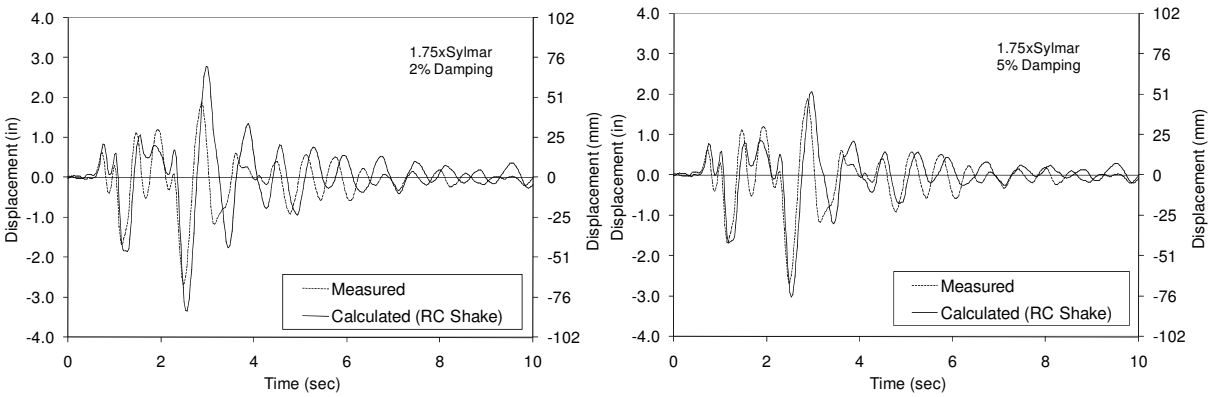

Figure 14. Measured and RC-shake results for 2% and 5% damping under 1.75 × Sylmar.

results for the 5% damping correlated better with the measured data than those for the 2% damping did. Review of Figures 14 and 12 shows that the performance of the SDOF model was comparable to that of the MDOF model.

6. Conclusions

The exploratory study presented in this article showed the feasibility of using carbon fiber laminate in combination with concrete for eventual application in highway bridge piers in which durability is of concern, and where steel reinforcement congestion is a problem. The measured shake table test data indicated that the target behavior was achieved with respect to shifting of the plastic hinge locations, linear response of members outside the plastic hinges, and the effectiveness of CFRP fabrics in keeping the bent cap and the joints damage free.

Comparison of the analytical and experimental results indicates that familiar constitutive relationships may be used to estimate the strength of concrete-carbon fiber laminate sections. However it should be noted that the computations are somewhat more involved than conventional structural engineering analyses.

Both the MDOF and the SDOF nonlinear response history analytical models with stiffness degradation led to a reasonably close agreement with the test data particularly when 2% viscous damping ratio was used. For the relatively simple, two-column test pier in which the fundamental mode essentially controlled the response no particular improvement of the response was evident when the MDOF model was used instead of the SDOF model.

Acknowledgements. The study presented in this article was funded by the National Science Foundation Grant CMS 980080. The support is gratefully acknowledged. The assistance of Dr. Nathan Johnson and Dr. Patrick Laplace in the experimental phase of the study is appreciated.

References

[Abdel-Fattah and Wight 1987] B. Abdel-Fattah and J. K. Wight, "Study of moving beam plastic hinging zones for earthquake-resistant design of reinforced concrete buildings", *ACI Struct. J.* **84**:1 (1987), 31–39.

[Galunic et al. 1977] B. Galunic, V. V. Bertero, and E. P. Popov, "An approach for improving seismic behavior of reinforced concrete interior joints", Technical Report UCB/EERC-77/30, Earthquake Engineering Research Center, University of California, Berkeley, CA, 1977, Available at http://nisee.berkeley.edu/elibrary/Text/81001486.

[Mirmiran et al. 2000] A. Mirmiran, M. Shahawy, C. El Khoury, and W. Naguib, "Large beam-column tests on concrete-filled composite tubes", *ACI Struct. J.* **97**:2 (2000), 268–276.

[Moustafa et al. 2004] K. Moustafa, D. Sanders, and M. Saiidi, "Impact of aspect ratio on two-column bent seismic performance", Technical Report CCEER-04-3, Center for Civil Engineering Earthquake Research, Department of Civil Engineering, University of Nevada, Reno, NV, February 2004.

[Prakash et al. 1994] V. Prakash, G. H. Powell, and S. D. Campbell, *DRAIN-3DX: base program description and user guide*, Version 1.10, Department of Civil Engineering, Univ. of California, Berkeley, CA, 1994, Available at http://nisee.berkeley.edu/elibrary/Text/300016.

[Reinhardt et al. 2003] E. Reinhardt, M. Saiidi, and R. Siddharthan, "Seismic performance of a CFRP/concrete bridge bent on flexible footings", Technical Report CCEER-03-4, Civil Engineering Department, University of Nevada, Reno, NV, August 2003.

[Saiidi 1982] M. Saiidi, "Hysteresis models for reinforced concrete", *J. Struct. Div.* (*ASCE*) **108**:5 (1982), 1077–1087.

[Saiidi et al. 1994] M. Saiidi, F. Gordaninejad, and N. Wehbe, "Behavior of graphite/epoxy concrete composite beams", *J. Struct. Eng.* (*ASCE*) **120**:10 (1994), 2958–2976.

[Saiidi et al. 2002] M. Saiidi, B. Gopalakrishnan, and R. Siddharthan, "Shake table studies of effects of foundation flexibility on seismic demand in substandard bridge piers", pp. 553–570 in *Innovations in design with emphasis on seismic, wind, and environmental loading: quality control and innovations in materials/hot-weather concreting* (Cancún, 2002), edited by V. M. Malhotra, ACI Special Publication **209**, American Concrete Institute, Farmington Hills, MI, 2002. Report No. SP-209-30.

[Teng et al. 2001] J. G. Teng, J. F. Chen, S. T. Smith, and L. Lam, *FRP-strengthened RC structures*, Wiley, Chichester, 2001.

Received 8 Mar 2009. Revised 16 May 2009. Accepted 17 May 2009.

M. SAIID SAIIDI: saiidi@unr.edu
Department of Civil and Environmental Engineering, University of Nevada, Reno, NV 89557, United States

ERIK REINHARDT: ereinhardt22@yahoo.com
Halcrow-Yolles Structural Engineers, 5550 W Flamingo Road, Las Vegas, NV 89103, United States

FARAMARZ GORDANINEJAD: faramarz@unr.edu
Department of Mechanical Engineering (MS 312), University of Nevada, Reno, NV 89557, United States